Article

Electrochemical Gate-Controlled Conductance of Single Oligo(phenylene ethynylene)s

Xiaoyin Xiao, Larry A. Nagahara, Adam M. Rawlett, and Nongjian Tao

J. Am. Chem. Soc., **2005**, 127 (25), 9235-9240• DOI: 10.1021/ja050381m • Publication Date (Web): 01 June 2005

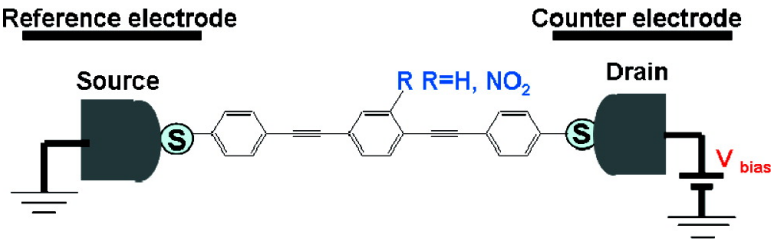

More About This Article

Additional resources and features associated with this article are available within the HTML version:

- Supporting Information
- Links to the 41 articles that cite this article, as of the time of this article download
- Access to high resolution figures
- Links to articles and content related to this article
- Copyright permission to reproduce figures and/or text from this article

View the Full Text HTML

Journal of the American Chemical Society is published by the American Chemical Society. 1155 Sixteenth Street N.W., Washington, DC 20036

J|A|C|S
ARTICLES
Published on Web 06/01/2005

Electrochemical Gate-Controlled Conductance of Single Oligo(phenylene ethynylene)s

Xiaoyin Xiao,[†] Larry A. Nagahara,[‡] Adam M. Rawlett,[§] and Nongjian Tao*,[†]

Contribution from the Department of Electrical Engineering and the Center for Solid State Electronics Research, Arizona State University, Tempe, Arizona 85287, Embedded Systems and Physical Sciences Lab, Motorola Labs, Tempe, Arizona 85284, and Multifunctional Materials Branch, U.S. Army Research Laboratory, APG, Maryland 21005

Received January 20, 2005; E-mail: nongjian.tao@asu.edu

Abstract: We have studied electron transport properties of unsubstituted oligo(phenylene ethynylene) (OPE) (**1**) and nitro-substituted OPE (**2**) covalently bound to two gold electrodes. The conductance values of single **1** and **2** are ~13 and ~6 nS, respectively. In addition to a decrease in the conductance, the presence of the nitro moiety leads to asymmetric *I*−*V* characteristics and a negative differential resistance-like (NDR-like) behavior. We have altered the nitro-substituted OPE by electrochemically reducing the nitro group and by varying the pH of the electrolyte. The conductance decreases linearly with the electron-withdrawing capability (i.e., Hammett substituent values) of the corresponding reduced species. In contrast, the conductance of **1** is independent of the pH and the electrode potential.

Introduction

The vision of using a single molecule or a small number of molecules to build electronic devices has led to a growing interest in molecular electronics in recent years.[1−6] One essential task in molecular electronics is to understand electron transport through a single molecule electrically wired to two electrodes.[7−16] This requires us to determine the dependence of the electron transport properties not only on temperature,[17] device geometry,[18−20] and molecule−electrode interfaces[21,22] but also on the chemical nature of the molecule, including substitution, redox properties, molecular length, and conjugation. The aim of the present work is to study the role of substitution on the conductance of single oligo(phenylene ethynylene)s (OPE) dithiolated molecules and to control the electron transport properties of the molecules via electrochemical reaction of the substituent groups.

OPE dithiolated molecules are attractive for molecular electronics due to several reasons. (1) The HOMO−LUMO gap of the molecules is ~3 eV, rather small in comparison to that of molecules with saturated bonds, which may lead to efficient electron transport. (2) The synthetic flexibility to alter their chemical moieties makes them good candidates for one to study the substituent effects on the electron transport properties.[23−29] For example, by controlling the electron donating and withdrawing of the substituents on the OPE, one expects a large

[†] Arizona State University.
[‡] Motorola Labs.
[§] U.S. Army Research Laboratory.

(1) Nitzan, A.; Ratner, M. A. *Science* **2003**, *300*, 1384−1389.
(2) Heath, J. R.; Stoddart, J. F.; Williams, R. S. *Science* **2004**, *303*, 1136−1137.
(3) Wassel, R. A.; Gorman, C. B. *Angew. Chem., Int. Ed.* **2004**, *43*, 5120−5123.
(4) Tour, J. M. *Acc. Chem. Res.* **2000**, *33*, 791−804.
(5) Salomon, A.; Cahen, D.; Lindsay, S.; Tomfohr, J.; Engelkes, V. B.; Frisbie, C. D. *Adv. Mater.* **2003**, *15*, 1881−1890.
(6) Park, J. et al. *Nature* **2002**, *417*, 722−725.
(7) Chen, J.; Reed, M. A.; Rawlett, A. M.; Tour, J. M. *Science* **1999**, *286*, 1550−1552.
(8) Kushmerick, J. G.; Lazorcik, J.; Patterson, C. H.; Shashidhar, R.; Seferos, D. S.; Bazan, G. C. *Nano Lett.* **2004**, *4*, 639−642.
(9) Smit, R. H. M.; Noat, Y.; Untiedt, C.; Lang, N. D.; van Hemert, M. C.; van Ruitenbeek, J. M. *Nature* **2002**, *419*, 906−909.
(10) Reichert, J.; Ochs, R.; Beckmann, D.; Weber, H. B.; Mayor, M.; Löhneysen, H. v. *Phys. Rev. Lett.* **2002**, *88*, 176804.
(11) Park, H.; Lim, A. K. L.; Alivisatos, A. P.; Park, J.; McEuen, P. L. *Appl. Phys. Lett.* **1999**, *75*, 301−303.
(12) Salomon, A.; Arad-Yellin, R.; Shanzer, A.; Karton, A.; Cahen, D. *J. Am. Chem. Soc.* **2004**, *126*, 11648−11657.
(13) Andres, R. P.; Bein, T.; Dorogi, M.; Feng, S.; Henderson, J. I.; Kubiak, C. P.; Mahoney, W.; Osifchin, R. G.; Reifenberger, R. *Science* **1996**, *272*, 1323−1325.
(14) Gittins, D. I.; Bethell, D.; Schiffrin, D. J.; Nichols, R. J. *Nature* **2000**, *408*, 67−69.
(15) Cui, X. D.; Primak, A.; Zarate, X.; Tomfohr, J.; Sankey, O. F.; Moore, A. L.; Moore, T. A.; Gust, D.; Harris, G.; Lindsay, S. M. *Science* **2001**, *294*, 571−574.
(16) Xu, B. Q.; Tao, N. J. *Science* **2003**, *301*, 1221−1223.
(17) Selzer, Y.; Cabassi, M. A.; Mayer, T. S.; Allara, D. L. *J. Am. Chem. Soc.* **2004**, *126*, 4052−4053.
(18) Guisinger, N. P.; Greene, M. E.; Basu, R.; Baluch, A. S.; Hersam, M. C. *Nano Lett.* **2004**, *4*, 55−59.
(19) Le, J. D.; He, Y.; Hoye, T. R.; Mead, C. C.; Kiehl, R. A. *Appl. Phys. Lett.* **2003**, *83*, 5518−5520.
(20) Wassel, R. A.; Credo, G. M.; Fuierer, R. R.; Feldheim, D. L.; Gorman, C. B. *J. Am. Chem. Soc.* **2004**, *126*, 295−300.
(21) Cai, L. T.; Skulason, H.; Kushmerick, J. G.; Pollack, S. K.; Naciri, J.; Shashidhar, R.; Allara, D. L.; Mallouk, T. E.; Mayer, T. S. *J. Phys. Chem. B* **2004**, *108*, 2827−2832.
(22) Beebe, J. M.; Engelkes, V. B.; Miller, L. L.; Frisbie, C. D. *J. Am. Chem. Soc.* **2002**, *124*, 11268−11269.
(23) Luo, Y.; Wang, C. K.; Fu, Y. *J. Chem. Phys.* **2002**, *117*, 10283−10290.
(24) Selzer, Y.; Salomon, A.; Ghabboun, J.; Cahen, D. *Angew. Chem., Int. Ed.* **2002**, *41*, 827−830.
(25) Mayor, M.; Weber, H. B.; Reichert, J.; Elbing, M.; von Hanisch, C.; Beckmann, D.; Fischer, M. *Angew. Chem. Int. Ed.* **2003**, *42*, 5834−5838.
(26) Chen, H.; Lu, J. Q.; Wu, J.; Note, R.; Mizuseki, H.; Kawazoe, Y. *Phys. Rev. B* **2003**, *67*, 113408.
(27) Bauschlicher, C. W.; Lawson, J. W.; Ricca, A.; Xue, Y. Q.; Ratner, M. A. *Chem. Phys. Lett.* **2004**, *388*, 427−429.
(28) Taylor, J.; Brandbyge, M.; Stokbro, K. *Phys. Rev. B* **2003**, *68*, 121101.
(29) Vedova-Brook, N.; Matsunaga, N.; Sohlberg, K. *Chem. Phys.* **2004**, *299*, 89−95.

change in the conductance.[23,29] (3) OPE−NO_2 exhibits interesting negative differential resistance (NDR)[7,30−33] and stochastic conductance switching phenomena.[34−38] (4) OPE−NO_2 is electroactive, which allows one to change the substituent via electrochemical reduction of the nitro group.

Many previous experiments on OPE molecules involved either a large number of molecules or only one end covalently attached to one electrode.[7,32,39] We report here on a study of the electron transport properties of single OPEs covalently attached to two electrodes using a scanning tunneling microscopy (STM)-break junction method. Furthermore, we determine the dependence of the single molecule conductance as a function of the electrochemical gate voltage.

Experimental Section

Materials and Measurements. The STM-break junction method was described briefly in ref 16. Here, we provide more details. The setup is modified from Pico-STM (Molecular Imaging). In the present work, we used a gold substrate and a gold tip. The substrate was prepared by thermally evaporating 100 nm gold on mica in a UHV chamber. Prior to each experiment, the substrate was briefly annealed in a hydrogen flame. The STM tip was prepared by cutting a 0.25 mm gold wire (99.999%), which was then coated with Apiezon wax in order to reduce ionic conduction and polarization currents. The leakage current, due to ionic conduction and polarization, was on the order of picoamperes. The STM cell was cleaned by piranha solution (98% H_2SO_4:30% H_2O_2 = 3:1, v/v) and then sonicated in 18 MΩ water three times. (Caution: piranha solution reacts violently with most organic materials and must be handled with extreme care.) The electrochemical experiment was conducted in an argon atmosphere. The potentials of the tip and the substrate were controlled with respect to a quasi reference electrode (Ag wire) using a gold counter electrode and a bipotentiostat (PicoStat, Molecular Imaging). The quasi reference electrode was calibrated against the more commonly used Ag/AgCl (in 3.5 M KCl) reference electrode.

The first step of the conductance measurement is to image the substrate covered with OPE molecules in solution. The STM image reveals typically sharp monatomic steps and well-ordered molecular domain structures of the adsorbed molecules. After imaging the substrate, we turn off the STM feedback and control the tip movement using a separate computer running a Labview program. The program detects the conductance between the tip and the substrate and compares it to a preset value (e.g., $4G_0$, where $G_0 = 2e^2/h \sim 77\ \mu$S, where e is the electron charge and h is the Planck constant). If the conductance is smaller than the preset value, the program drives the z-piezo of the STM scanner to move the tip linearly toward the substrate to form a quantum point contact. The driving rate of the STM tip is usually set at around 40 nm/s. If the conductance is greater than the preset value, the program moves the tip out of the contact until the current drops to zero and then moves the tip back toward the substrate to re-establish the preset value. In this way, the tip is driven in to and out of contact with the substrate repeatedly, and the transient conductance curves (Figure 1b) are recorded with a digital oscilloscope during the process. Drift often moves the tip either too close to the substrate or too far from the substrate. When this occurs, we switch it back to the STM feedback control, which moves the tip back to the tunneling regime. Many transient conductance curves, such as the ones shown in Figure 1b, are recorded and then analyzed with a separate Labview program. The program selects the ones with stepwise features and generates a conductance histogram (e.g., Figure 1c). The percentage of the curves with clear steps varies from 20−40%, depending on the samples. Conductance histogram of the curves reveals pronounced peaks located at integer multiples of a fundamental conductance value which is identified as the conductance of a single molecule.[7−16] When we measure the conductance of a new molecule, the gain of the commercial current amplifier has to be adjusted to cover a current range varying from microamperes to tens of picoamperes until a proper gain is found.

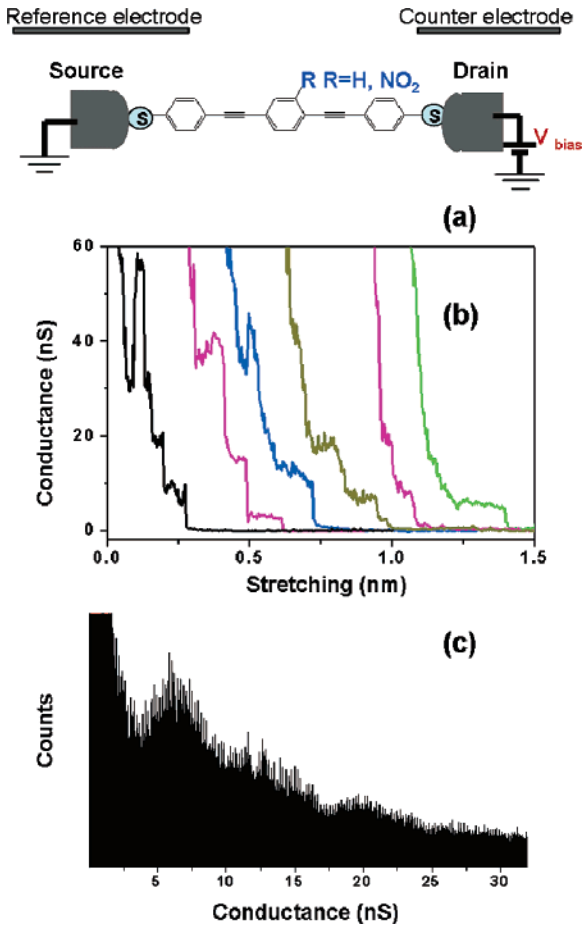

Figure 1. (a) Schematic illustration of a single molecular junction and (b and c) the individual conductance curves with corresponding conductance histogram constructed from 320 similar curves.

Once the conductance of the molecule is determined using the conductance histogram approach, we then use the following procedures to measure the $I-V$ curves of single molecules. First, the STM tip is brought within the tunneling range of the substrate using the commercial STM controller. We then turn off the feedback and move the tip in to and out of contact with the substrate by manually adjusting a voltage applied to the z-piezo of the STM scanner. Once the conductance drops to a conductance step corresponding to the single molecule conductance (determined by the statistical method), we freeze the STM tip position and perform the $I-V$ measurements. This approach is useful, but it requires extremely good STM stability. We can routinely hold the tip for many seconds to a few minutes using our setup.

(30) Kratochvilova, I.; Kocirik, M.; Zambova, A.; Mbindyo, J.; Mallouk, T. E.; Mayer, T. S. *J. Mater. Chem.* **2002**, *12*, 2927−2930.
(31) Rawlett, A. M.; Hopson, T. J.; Nagahara, L. A.; Tsui, R. K.; Ramachandaran, G. K.; Lindsay, S. M. *Appl. Phys. Lett.* **2002**, *81*, 3043−3045.
(32) Fan, F. R. F.; Yang, J. P.; Cai, L. T.; Price, D. W.; Dirk, S. M.; Kosynkin, D. V.; Yao, Y. X.; Rawlett, A. M.; Tour, J. M.; Bard, A. J. *J. Am. Chem. Soc.* **2002**, *124*, 5550−5560.
(33) Walzer, K.; Marx, E.; Greenham, N. C.; Less, R. J.; Raithby, P. R.; Stokbro, K. *J. Am. Chem. Soc.* **2004**, *126*, 1229−1234.
(34) Ramachandran, G. K.; Hopson, T. J.; Rawlett, A. M.; Nagahara, L. A.; Primak, A.; Lindsay, S. M. *Science* **2003**, *300*, 1413−1416.
(35) Donhauser, Z. J. et al. *Science* **2001**, *292*, 2303−2307.
(36) McCreery, R.; Dieringer, J.; Solak, A. O.; Snyder, B.; Nowak, A. M.; McGovern, W. R.; DuVall, S. *J. Am. Chem. Soc.* **2003**, *125*, 10748−10758.
(37) Wassel, R. A.; Fuierer, R. R.; Kim, N. J.; Gorman, C. B. *Nano Lett.* **2003**, *3*, 1617−1620.
(38) Khondaker, S. I.; Yao, Z.; Cheng, L.; Henderson, J. C.; Yao, Y. X.; Tour, J. M. *Appl. Phys. Lett.* **2004**, *85*, 645−647.
(39) Kushmerick, J. G.; Naciri, J.; Yang, J. C.; Shashidhar, R. *Nano Lett.* **2003**, *3*, 897−900.

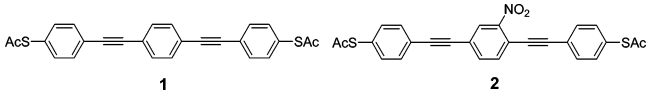

1 **2**

For this study, we focused on compounds **1** and **2**. The latter is electroactive and has been shown to exhibit NDR effects. We synthesized the OPE compounds according to the protocol published previously[40] and characterized by mass spectroscopy and NMR for both proton and carbon. The purity was about 99%. OPEs were self-assembled on the gold substrate by a base-promoted adsorption.[41] The compound (1 mg) was dissolved in THF or acetonitrile (10 mL). After 10 min sonication and 10 min sparge with argon gas, the molecules were deprotected by adding 20 μL of NaOH (0.2 M). The gold substrate was immersed into the sample solution at room temperature for a short period (less than 4 h). The argon-saturated solution was immediately covered with aluminum foil to avoid light exposure during self-assembly. The substrate was then thoroughly rinsed with ethanol and dried in the nitrogen atmosphere. Conventional cyclic voltammetry was carried out on Au bead electrodes (99.999%) in an acetonitrile solution containing tetrabutylamine perchlorate (TBAP) as the supporting electrolyte. We used the redox peaks of Fc^+/Fc as an internal potential standard to calibrate the potential in the organic electrolyte. In aqueous electrolytes, we calibrate the electrode potential using the redox potential of $[Fe(CN)_6]^{3-}/[Fe(CN)_6]^{4-}$ (see Supporting Information). Anhydrous THF (Aldrich) and anhydrous acetonitrile (Aldrich) were used after distillation. The remaining chemicals (NaOH, $NaClO_4$, and TBAP) were analytical grade and used as received. All measurements were carried out at room temperature, ~20 °C.

Results and Discussion

A. Single Molecule Conductance. Our first objective is to determine the single molecule conductance of OPEs covalently attached to gold electrodes. Figure 1b shows a series of steps in the conductance curves for compound **2**. These conductance steps are due to the formation of 1, 2, 3, ... OPE molecules in the junctions. There is a considerable amount of variations in the conductance steps from one molecular junction to another, as shown in the spread in the histogram (Figure 1c), possibly due to different microscopic details of the individual junctions. Nevertheless, the conductance histogram constructed from 320 curves shows pronounced peaks near the integer multiple of a fundamental value for the molecule. The fundamental value gives a well-defined average conductance of a single molecule. In this case for compound **2**, the conductance is ~6 nS. Similarly, hundreds of conductance curves were obtained for compound **1**, yielding a conductance of ~13 nS. The presence of the nitro group decreases the conductance of **1** by a factor of ~2.

The conductance values are on the same order of magnitude as those measured using cross-wire[39] and close to those obtained by the electromigrated junction[42] and mechanical break junction methods.[10] However, one has to be cautious when making such comparisons since we determine the *average* conductance of *single* molecules while the numbers of molecules in the previous measurements were not defined. The conductance of **2** obtained by conducting AFM is on the order of picosiemens. This difference might be due to imperfect contact between the nanoparticles and the AFM probe, or the fact that the AFM measured molecules that were embedded in a matrix of an organic monolayer.[31]

B. NDR-like Effect. Once the conductance of a single molecule is firmly established using the statistical analysis, we used our second method to measure $I-V_{bias}$ characteristics of single molecule junctions. For molecules **1** and **2**, we determined that within a relative small bias voltage range, the $I-V_{bias}$ curve can be reproducibly obtained by cycling the bias voltage between −1.5 and +1.5 V for several cycles (Figure 2a,b), then the current suddenly drops to zero, corresponding to the breakdown of the molecular junction at the molecule−electrode interfaces, or occasionally jumps to a higher value relating to the attachment of two molecules. When the V_{bias} range is greater than ~1.5 V, the current becomes increasingly noisy, which may be due to voltage-induced structural changes in molecular junction or a local heating effect.[43]

There are significant differences in the $I-V_{bias}$ curves between molecules **1** and **2**. First, the slope of the $I-V_{bias}$ curves near zero bias for **1** is about 2-fold larger as that for **2**, which is due to different conductance of the two molecules. Second, the $I-V_{bias}$ curves for **1** are symmetric, while the $I-V_{bias}$ curves for **2** are rather asymmetric. The asymmetric $I-V_{bias}$ curves are correlated with the asymmetric position of NO_2 group of **2**. An interesting observation is that the polarity of the asymmetric $I-V_{bias}$ curves varies from one junction to another, demonstrating the random orientation of a single molecule trapped in the junction.[44,45] Third, 90% of the $I-V_{bias}$ curves for **2** show distinct sharp current peaks between 1 and 2 V, which resembles the NDR effect. In contrast, 85% of $I-V_{bias}$ curves of **1** are rather smooth, while the remaining 15% of the curves show some small current spikes (Figure 2c) at large bias (~1.5 V), which are likely due to bias voltage-induced instability in the molecular junctions.

Two typical $I-V_{bias}$ curves are plotted in Figure 2d. The bias voltage is repeatedly swept between −2 and +2 V, starting from −2 V. The NDR-like peaks occur at both positive and negative bias voltages, but their PVRs (peak-to-valley ratio) are quite different. The appearance of the NDR-like peak in both positive and negative bias voltages in the same molecular junction rules out the possibility that the NDR-like peak is due to the reduction of S−Au, which would cause breakdown of the single molecule junction in the present case.[12] Typically, the PVR on the high current side is significantly larger than that on the low current side. Since the asymmetric $I-V_{bias}$ curves are correlated with the asymmetric location of the nitro moiety, the asymmetric PVR demonstrates that the NDR-like effect is related to the electroactive nitro moiety.

The NDR-like peaks usually either decrease or diminish in the reverse voltage sweep, indicating that a possible irreversible redox process is involved. Figure 3 is an example that shows NDR-like peaks in both forward and reverse potential scan directions. The NDR-like peak appears at 1.85 V in the forward positive scan direction, and it shifts to ~2 V in the reverse direction. The junction usually breaks down when the bias is swept above +2 V or below −2 V. One such example is shown in the inset of Figure 3. The breakdown of the molecular

(40) Tour, J. M. et al. *Chem.−Eur. J.* **2001**, *7*, 5118−5134.
(41) Cheng, L.; Yang, J. P.; Yao, Y. X.; Price, D. W.; Dirk, S. M.; Tour, J. M. *Langmuir* **2004**, *20*, 1335−1341.
(42) Selzer, Y.; Cai, L. T.; Cabassi, M. A.; Yao, Y. X.; Tour, J. M.; Mayer, T. S.; Allara, D. L. *Nano Lett.* **2005**, *5*, 61−65.
(43) Chen, Y.-C.; Zwolak, M.; Di Ventra, M. *Nano Lett.* **2003**, *3*, 1691−1694.
(44) Kornilovitch, P. E.; Bratkovsky, A. M.; Williams, R. S. *Phys. Rev. B* **2002**, *66*, 165436.
(45) Reichert, J.; Weber, H. B.; Mayor, M.; von Lohneysen, H. *Appl. Phys. Lett.* **2003**, *82*, 4137−4139.

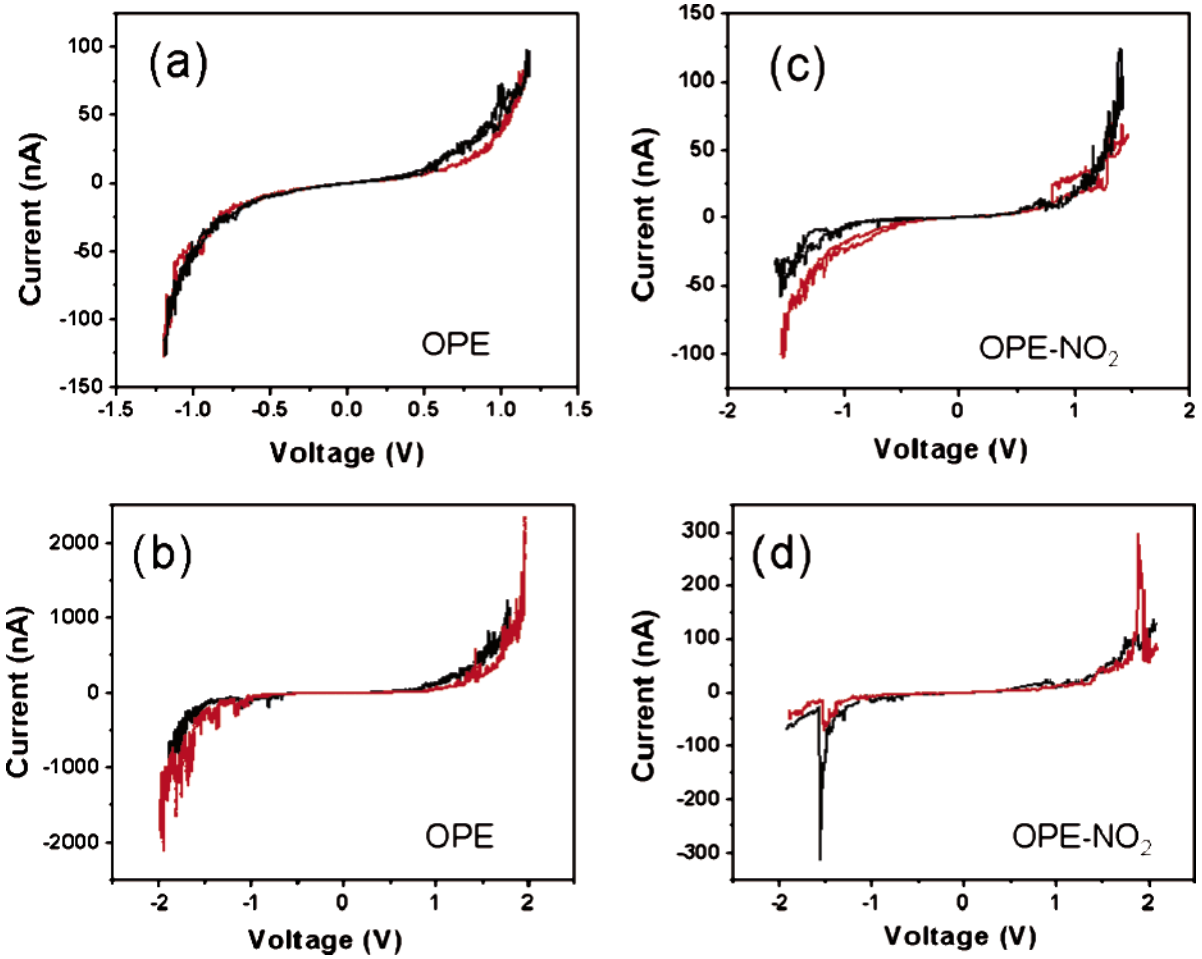

Figure 2. Individual current voltage ($I-V_{bias}$) curves for both molecules. (a and c) Reversible potential cycling below 1.5 V; (b and d) typical $I-V_{bias}$ curves recorded at a bias voltage below 2 V.

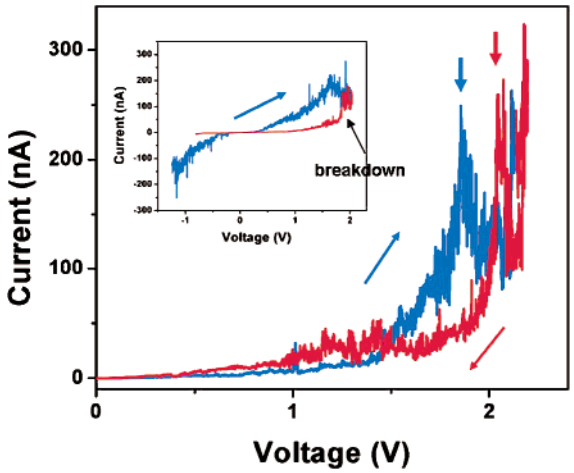

Figure 3. Two representative $I-V$ curves show the stability of the molecular junctions. Blue/red arrows point to the forward/reverse scan directions and the corresponding peaks, respectively.

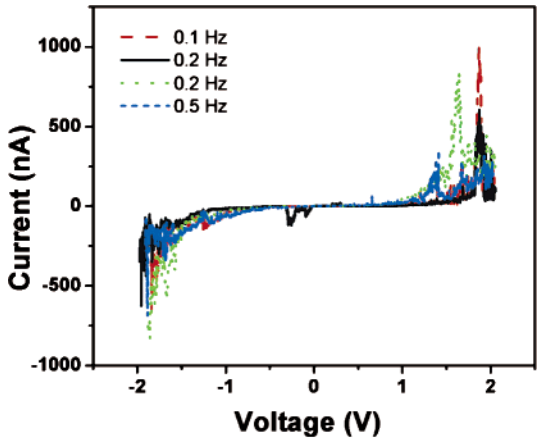

Figure 4. Influence of the scan rate on the NDR-like effect of individual single molecular junctions.

junction is visible as a sharp decrease of current to near zero, which is most likely due to the reductive desorption of Au−S bond.[46] Note that the NDR-like peaks are observed before the breakdown of the molecular junction. This observation, together with the fact (discussed below) that the nitro group is reduced at a more positive potential than the Au−S bond, further indicates that the NDR-like effect is associated with reduction of the nitro moiety rather than the reduction of the thiol.

To check if the NDR-like effect is due to a capacitive charging process, we recorded the $I-V$ characteristics at various bias sweep rates (Figure 4). We found that both the peak height and position vary from one molecular junction to another even at the same bias sweep rate, which shows that the NDR-like effect is sensitive to the microscopic detail of the individual molecular junctions. However, we did not observe a systematic dependence of the peak height on the sweep rate, which rules out the NDR-like effect as a simple capacitance charging process.

C. Potential-Controlled Conductance of OPEs. The results presented above were obtained in toluene, which did not allow us to control the electrochemical reaction of the molecules. To control the electrochemical reaction, we performed the measurements in electrolytes and under electrochemical condition. Using a bipotentiostat, we controlled the potentials of both the tip and the substrate electrodes, which can be operated in a fashion similar to a field effect transistor (FET). In a conventional solid state FET, a gate electrode controls the current between a source and a drain electrode via changing the carrier density. In contrast, the electrochemical gate controls the current through a molecule via electrochemically oxidizing or reducing the molecule, which has been observed for conducting polymer junctions.[47−50]

Figure 5a shows the cyclic voltammograms of thioacetate-protected OPEs on gold electrodes in anhydrous acetonitrile containing TBAP as the supporting electrolyte. In the case of **1**, only a small double layer charging current was observed. However, three reduction peaks near −0.8, −1.5, and −1.9 V were observed for **2**. The reduction peaks, $\mathbf{C}_1$ and $\mathbf{C}_2$, are similar to those observed by Reed et al.,[51] which are assigned to the electrochemical reduction of the nitro group. The third peak, $\mathbf{C}_3$, however, is due to the reductive desorption of the adsorbed molecules because it diminishes with potential cycles. Figure 5b shows the first potential cycle for deprotected **1** and **2**, while a small amount of NaOH aqueous solution was added to the above electrolyte. The reduction peaks at −1.16 V in both cases are due to molecular desorption, whereas the additional reduction peaks, near −0.5 and −1.1 V, are apparently due to the reduction of the nitro moiety in **2**. Note that the reduction processes are positively shifted and become almost irreversible in comparison to that shown in Figure 5a, demonstrating the role of water molecules involved in the reduction processes. The reduction potentials are shifted to more positive values in 0.1 M NaOH solution (Figure 5c).

We have measured the conductance of **1** and **2** at various electrode potentials between −0.9 and 0.3 V in 0.1 M NaOH solution. We held the potential at each value for 5 min and then performed the measurement with the STM-break junction according to the procedures described earlier. For **1**, the conductance is independent of the electrode potential. However, the conductance of **2** is sensitive to the potential and increases as the potential is shifted more negatively (Figure 6). This potential-dependent conductance also depends on the pH of the electrolyte. We have measured the conductance of **2** in 0.1 M $NaClO_4$ and 0.1 M NH_4Ac, both have much lower pH than that of NaOH. At potentials more positive than the reduction potentials, the conductance is the same for the different electrolytes, indicating the solution pH has little effect on the conductance of **2** when the molecule is not reduced. However, when decreasing the potential below the reduction potentials in $NaClO_4$ and NH_4Ac, the conductance first increases and then decreases, which is different from that in NaOH. This difference is related to the protonation of the amine group in $NaClO_4$ and

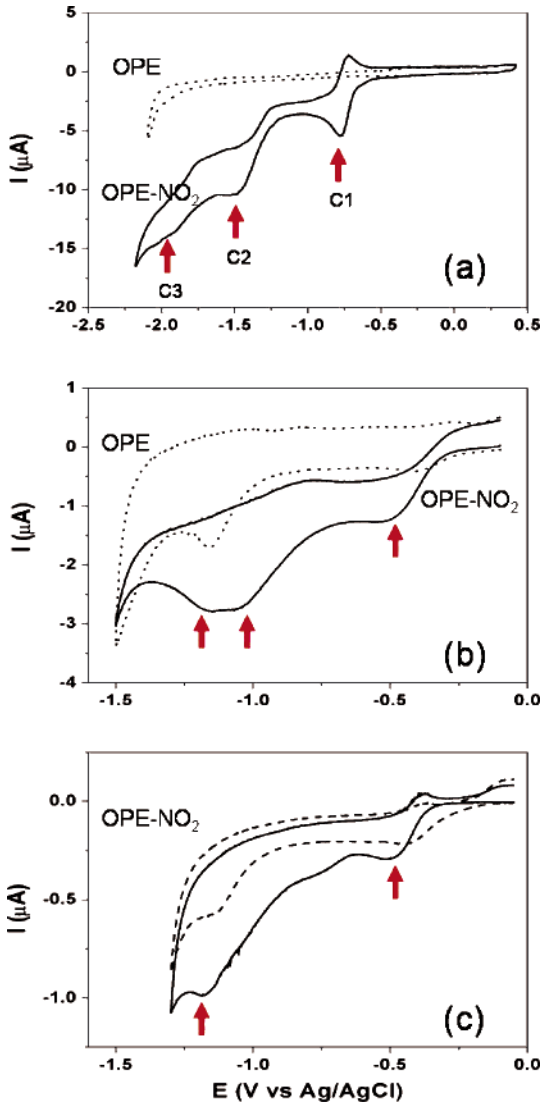

Figure 5. Voltammograms of OPEs on gold bead electrodes. (a) Thioacetate-protected **1** and **2** in anhydrous MeCN + 0.1 M TBAP solution, (b) thiol-deprotected **1** and **2** in MeCN/H_2O + 0.1 M TBAP + 0.001 M NaOH solution, (c) adsorbed **2** in 0.1 M NaOH solution (first two cycles). Sweep rate: 100 mV/s.

NH_4Ac, which indicates that OPE−NH_2 has a larger conductance value in basic solution than that in neutral solution. This conductance decrease of the final reduced molecules was also observed when the basic solution (0.1 M NaOH) was replaced by an acidic solution (0.1 M $HClO_4$).

The change in the conductance of molecule **2** upon electrochemical reduction is attributed to the changes of the substituent effect on the central benzene ring. The irreversible reduction of the nitro moiety in aqueous solutions gives rise to other substituents. The basic reduction process from $-NO_2$ to $-NH_2$ in aqueous medium can be described via a sequential reduction process through intermediate oxidation states: $-NO_2 \rightarrow -NO \rightarrow -NH(OH) \rightarrow -NH_2$.[52−54] Since the current ratio of the two reduction peaks in Figure 5b is approximately 1:2, we simply ascribe the reduction of **2** via a two-step reaction, that is, nitro

(46) Yang, G. H.; Liu, G. Y. *J. Phys. Chem. B* **2003**, *107*, 8746−8759.
(47) Meulenkamp, E. A. *J. Phys. Chem. B* **1999**, *103*, 7831−7838.
(48) Hulea, I. N.; Brom, H. B.; Houtepen, A. J.; Vanmaekelbergh, D.; Kelly, J. J.; Meulenkamp, E. A. *Phys. Rev. Lett.* **2004**, *93*, 166601.
(49) Chao, S. H.; Wrighton, M. S. *J. Am. Chem. Soc.* **1987**, *109*, 6627−6631.
(50) White, H. S.; Kittlesen, G. P.; Wrighton, M. S. *J. Am. Chem. Soc.* **1984**, *106*, 5375−5377.
(51) Chen, J.; Wang, W.; Reed, M. A.; Rawlett, A. M.; Price, D. W.; Tour, J. M. *Appl. Phys. Lett.* **2000**, *77*, 1224−1226.
(52) Rubinstein, I. *J. Electroanal. Chem.* **1985**, *183*, 379−386.
(53) Fan, L. J.; Wang, C.; Chang, S. C.; Yang, Y. W. *J. Electroanal. Chem.* **1999**, *477*, 111−120.
(54) Stapleton, J. J.; Harder, P.; Daniel, T. A.; Reinard, M. D.; Yao, Y. X.; Price, D. W.; Tour, J. M.; Allara, D. L. *Langmuir* **2003**, *19*, 8245−8255.

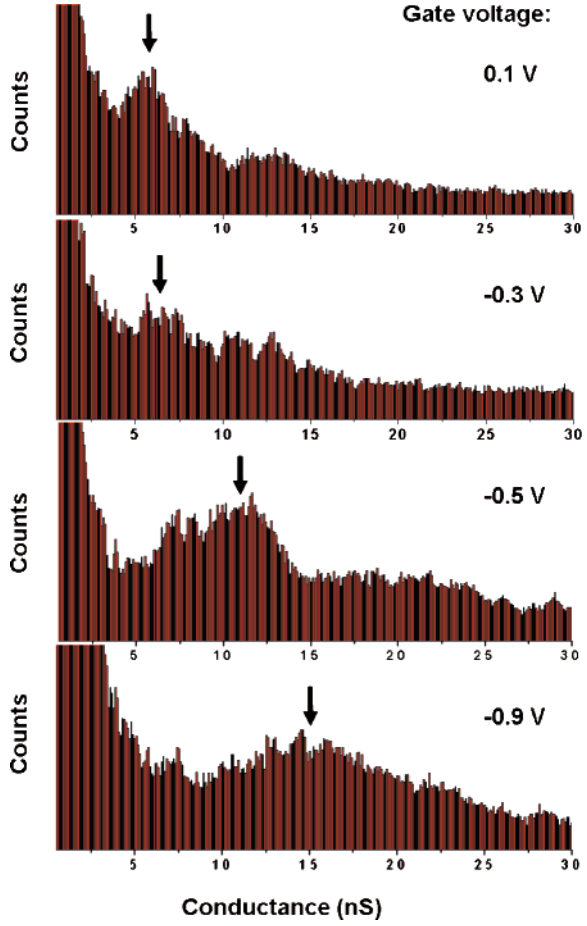

Figure 6. Conductance histograms of **2** at different electrode potentials in 0.1 M NaOH solution. The single molecular conductance value is marked by black arrows.

is reduced via a two-electron process at the first peak potential to nitroso (−NO) and is further reduced via a four-electron process to amine ($-NH_2$). Other products, such as hydroxylamine (−NH(OH)), may have been involved at intermediate negative potentials.

Hammett developed a set of substituent parameter values (σ), which correlate the electronic effect of substituents with the rates and equilibrium of organic reactions. The chemical nature of a substituent can shift the frontier molecular orbital and alter the electron transport efficiency through the molecule.[23,55] As shown in Figure 7, the measured conductance decreases linearly with σ, which is in good agreement with the theoretical estimation by Vedova-Brook et al.[29] The decrease of the conductance with σ is expected because large σ corresponds to a high electron-withdrawn substituent.[56] The plot of the conductance value versus reported the σ value shows linear relationship ($R \sim 0.93$) (Figure 7).

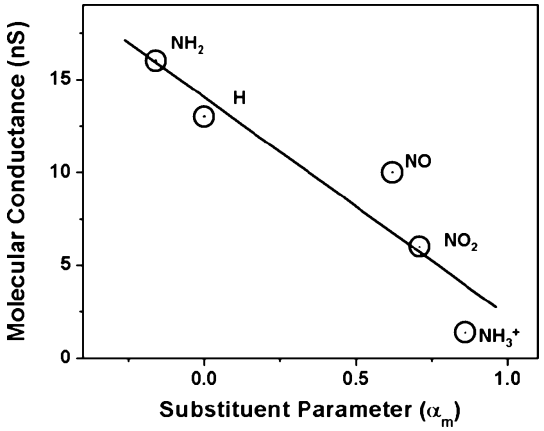

Figure 7. Plot of the observed conductance value versus substituent Hammett parameters.

Conclusion

We have studied electron transport properties of single **1** and **2** covalently bound to two gold electrodes in different solvents and electrolytes. The average single molecule conductance is 13 nS for **1** and ~6 nS for **2**. The $I-V_{bias}$ curves for **1** are symmetric and rather smooth. In contrast, the $I-V_{bias}$ curves for **2** are asymmetric and typically show an NDR-like effect. The asymmetry is due to the asymmetric position of the NO_2 group, and the NDR-like effect is related to an irreversible reaction of the NO_2 moiety. We have studied the two molecules under electrochemical control. For **1** that has no electroactivity within the studied potential range, the conductance is independent of the potential. **2** has two irreversible reduction reactions that occur in the NO_2 moiety, which leads to a change in the substituent and thus potential-dependent conductance. The conductance decreases linearly with the Hammett parameter, which describes the tendency of electron withdrawing from the conjugated molecule.

Acknowledgment. We thank NSF (CHE-0243423) for financial support.

Supporting Information Available: Cyclic voltammetry, UV spectroscopic data, and complete refs 6, 35, and 40. This material is available free of charge via the Internet at http://pubs.acs.org.

JA050381M

(55) Aviram, A.; Ratner, M. *Chem. Phys. Lett.* **1974**, *29*, 277−283.

(56) Hansch, C.; Leo, A.; Taft, R. W. *Chem. Rev.* **1991**, *91*, 165−195.